

# Semibatch Atom Transfer Radical Copolymerization of Styrene and Butyl Acrylate

Yao Fu, Michael F. Cunningham,\* Robin A. Hutchinson\*

**Summary:** Batch and semibatch butyl acrylate (BA) polymerizations are carried out using a heterogeneous atom transfer radical polymerization (ATRP) catalyst system, with excellent molecular weight (MW) control maintained at temperatures below 80 °C. A kinetic model, using rate coefficients from literature and catalyst solubility data from this study, provides a good representation of the experimental results, after modifying the model to account for the decrease in rate caused by intramolecular chain transfer. It is also demonstrated experimentally that well-defined random, gradient, and block styrene/BA copolymers can be synthesized by manipulating monomer feed profiles in the ATRP semibatch process.

**Keywords:** atom transfer radical polymerization; butyl acrylate; copolymerization; kinetics (polym.); modeling; styrene

## Introduction

Living radical polymerization (LRP) has emerged as a promising route for the synthesis of macromolecules with well-defined molecular weight, low polydispersities (often close to unity) and various architectures under mild conditions. Although much research has been focused on the synthesis of novel polymer structures not achievable with conventional free radical polymerization (FRP), there is little work examining the application of LRP under process conditions approaching those employed in industry. We have studied nitroxide mediated polymerization<sup>[1,2]</sup> and atom transfer radical polymerization (ATRP)<sup>[3]</sup> to synthesize polystyrene in a semibatch process typical of those used for production of low molecular weight solvent-borne polymers for application as automotive coatings resins. In addition, we have used a tubular ATRP reactor to elucidate the influence of a continuous

reaction process on conversion, molecular weight and polydispersity compared to batch polymerization experiments.<sup>[4]</sup> Continuous solution polymerization experiments of styrene and butyl acrylate (BA) were well-controlled, as evidenced by linear growth in the number average molecular weight ( $M_n$ ) with conversion and low polydispersity index (PDI).

ATRP, like other LRP systems, controls chain growth through a rapid equilibrium exchange between active radicals and dormant species, allowing slow but simultaneous growth of all chains while keeping the concentration of active radicals low to minimize termination. Maximum control is achieved if all chains are initiated immediately at the start of polymerization and if termination and other side reactions are completely suppressed. Meanwhile, the semibatch approach is often used industrially for FRP copolymerization because it permits good temperature control and superior control of copolymer composition. Combination of the two techniques – semibatch LRP – offers potential advantages to the coatings industry: the copolymer will have narrower PDI and lower viscosity for the same  $M_n$ , and improved chain uniformity will also reduce the

Department of Chemical Engineering, Dupuis Hall, Queen's University, Kingston, Ontario K7L 3N6, Canada

E-mail: michael.cunningham@chee.queensu.ca;  
robin.hutchinson@chee.queensu.ca

amount of expensive functionalized monomer that must be added. In this work, we turn our attention to combining ATRP chemistry with semibatch copolymerization, after first establishing suitable conditions for BA homopolymerization.

## Experimental Part

Styrene (99%, Aldrich), butyl acrylate (99%, Aldrich), toluene (99%, Aldrich), Cu(I)Br (98%, Aldrich), N,N,N',N'',N''-Pentamethyldiethylenetriamine (PMDETA, 99%, Aldrich), and methyl 2-bromopropionate (MBrP, 98%, Aldrich) were used as received. Batch and semibatch reactions were performed in a 1 L LabMax reactor system with an agitator and reflux condenser, and computer-controlled component feed rates and reactor temperature. A number of BA batch polymerizations were run at 90 °C using a BA/toluene 70/30 wt ratio and a molar ratio of 40:1:1:1 for [M]: [MBrP]: [CuBr]: [PMDETA], giving a theoretical polymer molecular weight of  $5100 \text{ g} \cdot \text{mol}^{-1}$  at 100% conversion. The batch experiments were run by adding initiator (MBrP), catalyst (CuBr), ligand (PMDETA) and monomer (BA) to the toluene solvent and then increasing the reaction temperature to 90 °C. Semibatch polymerization experiments were conducted using similar conditions as for the batch system, except with the majority of the total BA fed over a period of several hours. Semibatch BA/styrene copolymerization experiments were conducted in a similar fashion; in some cases (as described below), a fraction of the monomer was added to the initial precharge to the reactor, with the remainder added during the course of the polymerization.

Samples were taken at selected intervals, and analyzed for free monomer and polymer molecular weights. The residual monomer concentrations were determined using a Varian CP-3800 gas chromatograph (GC) setup, as detailed previously.<sup>[2–4]</sup> Calibration standards were constructed by mixing measured quantities of styrene and BA monomers into known mass of acetone, and

a linear calibration curve was constructed by plotting peak area versus monomer concentration.

A Waters 2698 Separation Module GPC with a set of four Styragel columns (HR4.0, HR3.0, HR1.0, HR0.5) was used to determine polymer average molecular weight and polydispersity (PDI). Tetrahydrofuran (THF) at 40 °C was used as the mobile phase at a flow of  $1 \text{ mL} \cdot \text{min}^{-1}$ , with polymer samples dissolved in THF to a concentration of 8 to  $10 \text{ mg} \cdot \text{mL}^{-1}$ . Two detectors were used to characterize the size of polymer chains after separation. Coupled with a Wyatt Technology Light Scattering (LS) detector, the output signal provides the absolute molar mass without the need for calibration standards but with knowledge of the  $dn/dc$  value. Coupled with the Waters 410 Differential Refractometer (RI) detector, the molecular weights are determined against a calibration curve constructed by analyzing 8 linear narrow PDI polystyrene standards ranging in molecular weight from 890 to  $3.55 \times 10^5 \text{ g} \cdot \text{mol}^{-1}$ . Molecular weights from the RI detector were recalculated for pBA homopolymer using literature<sup>[5]</sup> Mark-Houwink parameters of pS ( $K = 1.14 \times 10^{-4} \text{ dL} \cdot \text{g}^{-1}$ ,  $a = 0.716$ ) and pBA ( $K = 1.22 \times 10^{-4} \text{ dL} \cdot \text{g}^{-1}$ ,  $a = 0.700$ ). Normalization of the LS detector is obtained through a single narrow PDI polystyrene standard with molecular weight of  $3 \times 10^4 \text{ g} \cdot \text{mol}^{-1}$ ; the  $dn/dc$  value for pBA required for analysis by the LS detector is  $0.065 \text{ mL} \cdot \text{g}^{-1}$ .<sup>[6]</sup> There was excellent agreement between the two detectors. Results from the LS detector are used for the discussion of BA homopolymerization below, while results from both detectors are presented for the BA/styrene copolymers.

## Results and Discussion

### BA Batch Polymerization

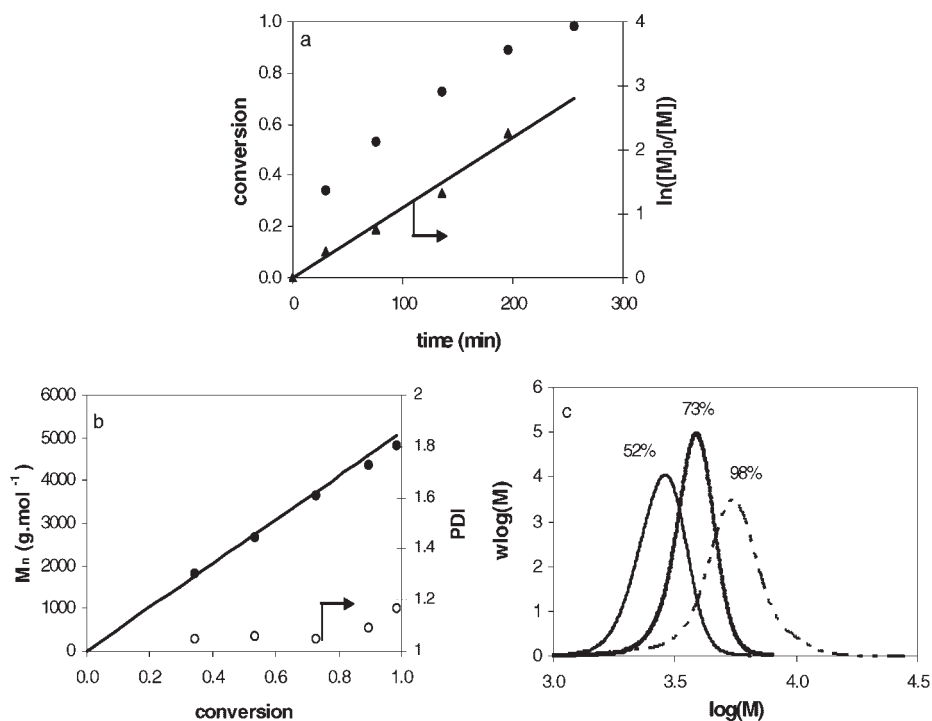
Before proceeding to the BA semibatch system, batch experiments were performed with 30 wt% toluene and a molar ratio of monomer: initiator: catalyst: ligand of

40:1:1:1. The reaction temperature of 90 °C is lower than that used for styrene<sup>[3]</sup> due to the faster activation kinetics and propagation of acrylates. Experimental results are shown in Figure 1. Almost complete monomer conversion is achieved in 4 h, with a linear relationship between  $\ln([M]_0/[M])$  and time indicating first-order kinetics with respect to monomer and a constant radical concentration during the batch polymerization. There is also a good linear relationship between  $M_n$  and conversion. PDI is very low (<1.2) at high conversion, showing that the system exhibits excellent control. The experimental molecular weights are in good agreement with the theoretical values, indicating that the initiator efficiency is close to unity, and the shift of the GPC traces with conversion indicates that there is no obvious loss of chains during the polymerization.

With CuBr/PMDETA, the catalyst complex is not completely soluble during

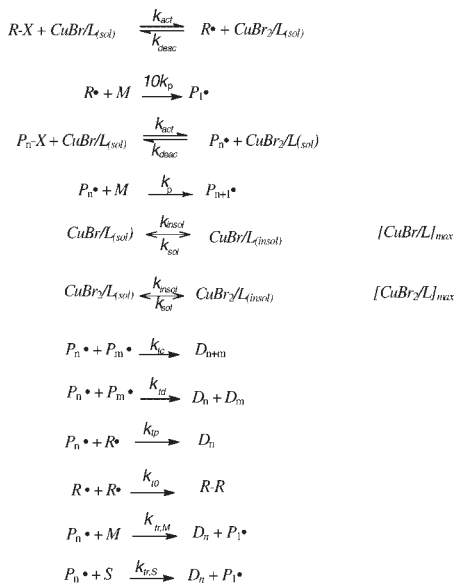
polymerization, such that the reaction system is heterogeneous. Previous studies have shown that only soluble Cu species participate in the mediation of chain growth.<sup>[3,7–10]</sup> We successfully modeled this effect for styrene ATRP assuming that an equilibrium between soluble and insoluble catalyst species is established once the limiting concentration of Cu-ligand complex ( $[CuBr/L]_{max}$  or  $[CuBr_2/L]_{max}$ ) in solution is reached.<sup>[3]</sup> Undissolved catalyst in the system, while not participating in the reaction, acts as a reservoir to maintain the Cu(II) to Cu(I) ratio relatively constant during the experiment. Atomic absorption spectroscopy was used to determine that Cu(I) solubility is five to ten times higher than that of Cu(II) for the PMDETA/Cu system.<sup>[3]</sup> The same approach is used here to represent the BA polymerization results.

Scheme 1 shows the basic mechanisms for BA ATRP (not including secondary reactions such as backbiting) implemented



**Figure 1.**

Batch ATRP of butyl acrylate at 90 °C with a BA:MBrP:CuBr:PMDETA molar ratio of 40:1:1:1: (a) conversion vs. time and  $\ln([M]_0/[M])$  vs. time; line is best linear fit of  $\ln([M]_0/[M])$  vs. time; (b) number average MW and PDI vs. conversion; line is theoretical  $M_n$ ; (c) MWDs at conversions indicated on the plot.

**Scheme 1.**

Kinetic mechanisms for butyl acrylate atom transfer radical polymerization.

in *Predici*<sup>®</sup>. The model contains reversible activation/deactivation of initiator ( $R-X$ ) and dormant polymer chains ( $P_n-X$ ), propagation, polymer chain termination, primary radical termination, chain transfer to monomer and solvent, and precipitation reactions between soluble and insoluble Cu species. Rate coefficients for the system are

**Table 1.**

Rate coefficients of butyl acrylate ATRP at 90 °C ( $T$  in K).

Coefficient/Parameter	Expression/Value
$K_{eq}[11]$	$1 \times 10^{-8}$
$k_{deac} \text{ (L} \cdot \text{mol}^{-1} \cdot \text{s}^{-1})[12]$	$8 \times 10^7$
$k_{act} \text{ (L} \cdot \text{mol}^{-1} \cdot \text{s}^{-1})$	$0.8 (=K_{eq} \times k_{deac})$
$k_p \text{ (L} \cdot \text{mol}^{-1} \cdot \text{s}^{-1})[13]$	$2.21 \times 10^7 \exp(-2153/T)$
$k_t \text{ (L} \cdot \text{mol}^{-1} \cdot \text{s}^{-1})[14,15]$	$2.57 \times 10^8 \exp(-292/T)$
$k_{td} = 0.1k_t$ ; $k_{tc} = 0.9k_t$	
$k_{tr,m}/k_p[16]$	$0.016 \exp(-1830/T)$
$k_{tr,s}/k_p[15]$	$3.9 \exp(-3870/T)$
$\rho_{mon} \text{ (g} \cdot \text{cm}^{-3})[5]$	$0.9211 - 1.0 \times 10^{-3}(T-273.15)$
$\rho_{pol} \text{ (g} \cdot \text{cm}^{-3})[5]$	1.05
$k_{tp} \text{ (L} \cdot \text{mol}^{-1} \cdot \text{s}^{-1})[17]$	$1.0 \times 10^9$
$k_{to} \text{ (L} \cdot \text{mol}^{-1} \cdot \text{s}^{-1})[17]$	$2.5 \times 10^9$
$k_{sol} \text{ (s}^{-1})[7]$	1000
$k_{insol} \text{ (s}^{-1})[7]$	1000
$[CuBr/L]_{max} \text{ (mol} \cdot \text{L}^{-1})[18]$	0.028
$[CuBr_2/L]_{max} \text{ (mol} \cdot \text{L}^{-1})[18]$	0.006

taken from the literature, as summarized in Table 1. The value for  $K_{eq}$  ( $1 \times 10^{-8}$ ) is from an ATRP study using  $CuBr/PMDETA$  as catalyst for methyl acrylate at 100 °C,<sup>[11]</sup> and  $k_{deac}$  ( $8 \times 10^7 \text{ L} \cdot \text{mol}^{-1} \cdot \text{s}^{-1}$ ) is for a similar ATRP system at 90 °C.<sup>[12]</sup> The propagation rate constant of BA,  $k_p$ , was obtained by pulsed-laser polymerization<sup>[13]</sup> and is greater than styrene  $k_p$  by ~60 times at 90 °C. Termination can occur by combination (rate coefficient  $k_{tc}$ ) or disproportionation ( $k_{td}$ ), with combination dominant for polymerization of BA. Transfer can occur to monomer ( $k_{tr,M}$ ) and to solvent ( $k_{tr,S}$ ). The heterogeneity of the catalyst in the BA/toluene system is represented by the precipitation reactions between soluble and insoluble  $CuBr$  and  $CuBr_2$  species, as also used to represent the styrene system.<sup>[3]</sup> The values of  $k_{sol}$  and  $k_{insol}$  were chosen as  $10^3 \text{ s}^{-1}$  in order to keep the dynamics fast,<sup>[7]</sup> with the concentrations of the soluble/insoluble  $CuBr/CuBr_2$  species controlled by  $[CuBr/L]_{max}$  and  $[CuBr_2/L]_{max}$ , set according to experiments. These solubility values were obtained using atomic absorption spectroscopy, as described previously for styrene ATRP with the same catalyst system.<sup>[3]</sup> The solubility of both  $CuBr$  and  $CuBr_2$  are only slightly higher in an BA/toluene mixture compared to styrene/toluene at the same temperature, despite the higher polarity of acrylate compared to styrene.<sup>[18]</sup>

However, the basic ATRP and BA kinetic mechanisms of Scheme 1 fail to adequately represent the system, as shown in Figure 2. Experimentally conversion approaches 100% at 4 h, while the simulation reaches full conversion at the end of 30 min. To explore possible explanations for this difference, it is useful to examine the expression for polymerization rate:

$$R_p = k_p [M] K_{eq} \frac{[R-X][CuBr/L]_{sol}}{[CuBr_2/L]_{sol}} \quad (1)$$

In the equation,  $[R-X]$  is known experimentally from the amount of  $MBRP$  added, and  $[CuBr/L]_{max}$  and  $[CuBr_2/L]_{max}$  are set according to the experimental data. The

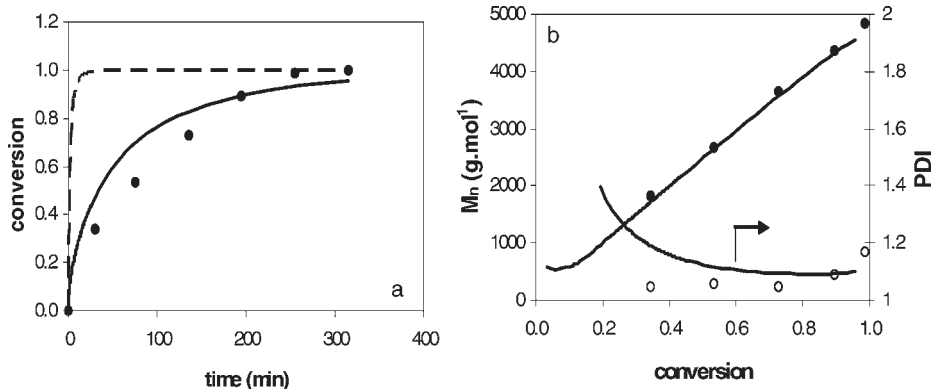


**Figure 2.**

Results for butyl acrylate ATRP batch polymerization: (a) conversion vs. time; (b) number average MW (closed symbols) and PDI (open symbols) vs. conversion. Data points indicate experimental measurements; the lines are model predictions generated via computer simulation with Table 1 coefficients (dashed line) and with reduced  $k_p$  (solid line).

remaining coefficients that may cause such a rapid polymerization rate in the simulation are  $k_p$  and  $K_{eq}$ . Although there is some uncertainty in  $K_{eq}$  estimates,<sup>[19,20]</sup> the large decrease required to match the rate data is not plausible. Thus, decreasing the propagation rate coefficient remains the only reasonable way to slow the reaction rate to match experiment. A decrease in effective propagation rate is in agreement with literature that concludes that intramolecular chain transfer (backbiting) produces midchain radicals that have much lower monomer addition rates.<sup>[13,15,21]</sup> Decreasing  $k_p$  to 1/7 of the original value provides a good fit of conversion and  $M_n$ , and the final PDI also is in agreement with experiment (Figure 2). It should be noted that the midchain radical structure should have a different activation/deactivation equilibrium with catalyst than the chain-end radical. Although it may be hypothesized that this equilibrium should be similar to methacrylates (due to the similar structure), this added complexity will not be considered further in this work. Thus, rigorous parameter estimation techniques were not used to obtain the fit shown in Figure 2.

The other possible reason that the basic mechanistic set of Scheme 1 fails to adequately represent the system is that it

neglects chain transfer between the ligand PMDETA and acrylate radical. This mechanism has been recently postulated based upon experiments observing retardation of polymerization rate with increasing PMDETA concentration.<sup>[22,23]</sup> Sharma et al.<sup>[24]</sup> use electron density functional theory to further explore this transfer mechanism. The calculations indicate that the proton abstraction from the PMDETA ligand occurs predominantly at a specific site of the molecule and, once generated, the ligand radical does not participate in any further chain-growth reactions.<sup>[24]</sup> However, the exact mechanism and rate coefficients for transfer to ligand are unknown, and the mechanism will not be considered further in this work.

### BA Semibatch Polymerization

The first ATRP semibatch experiment was run by charging toluene into the reactor and increasing the reaction temperature to 90 °C, then adding catalyst (CuBr), ligand (PMDETA), about 7% of the total BA and initiator (MBrP) before proceeding with the 6-hour addition of the remaining BA. The molar ratio of total monomer: initiator: catalyst: ligand was 40:1:1:1 with a target molecular weight of 5100 g·mol<sup>-1</sup>, the same as for the batch polymerization. The

system is heterogeneous and the reaction behaviour is similar to that observed for styrene semibatch ATRP.<sup>[3]</sup> A good linear relationship between  $M_n$  and conversion was found, as shown in Figure 3. However, PDI increased with conversion, climbing to a final value of 1.6 at 97% conversion, showing that the system lost control towards the end of the reaction. The experimental molecular weight is slightly higher than the target (theoretical) value of  $5100 \text{ g} \cdot \text{mol}^{-1}$ , indicating an initiator efficiency of about 0.68. The polymerization rate is much higher than that found for styrene ATRP at  $110^\circ\text{C}$ ; monomer conversion reached 90% at the end of the feeding time (360 minutes), whereas styrene conversion at  $110^\circ\text{C}$  was only 50% at the same time.<sup>[3]</sup> Free radical polymerization of BA was performed with *tert*-butyl peroxyacetate initiator at  $138^\circ\text{C}$ , using the same semibatch procedure, with initiator (2 wt%

relative to monomer) also fed continuously over a 6 h period. Figure 3 indicates that the time conversion profile for the ATRP experiment at  $90^\circ\text{C}$  is very similar to this starved-feed FRP reactor, although the concentration of free monomer in the reactor reaches slightly higher levels. The expected difference in  $M_n$  vs. conversion profile is observed between the FRP and ATRP experiments, although the final PDI of the ATRP experiment climbs to almost the same as that measured for FRP.

The BA model provided a reasonable description of the batch experimental results at  $90^\circ\text{C}$ , with  $k_p$  decreased from the literature (chain-end) value by a factor of 7. The same set of mechanisms and rate coefficients has been used to simulate the semibatch system, with results shown in Figure 4. The predicted reaction rate is slower than that measured experimentally, and predicted MW and PDI values are

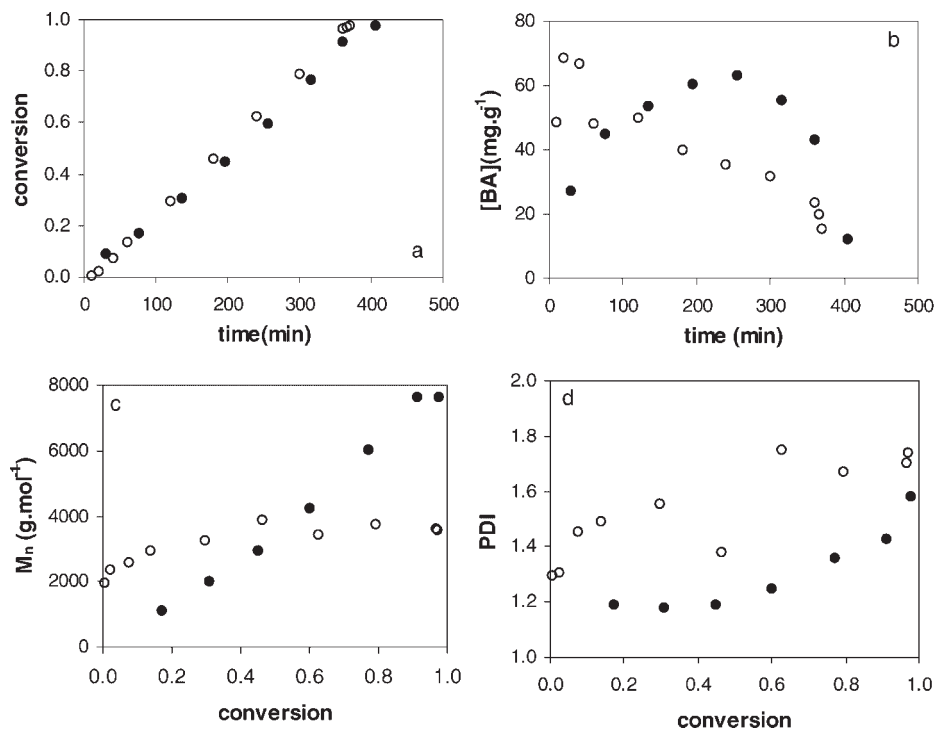


**Figure 3.**

Comparison between butyl acrylate semibatch ATRP (closed symbols) at  $90^\circ\text{C}$  and semibatch FRP (open symbols) at  $138^\circ\text{C}$ : (a) conversion vs. time; (b) [BA] ( $\text{mg} \cdot \text{g}^{-1}$ ) vs. time; (c) number average MW vs. conversion; (d) PDI vs. conversion.

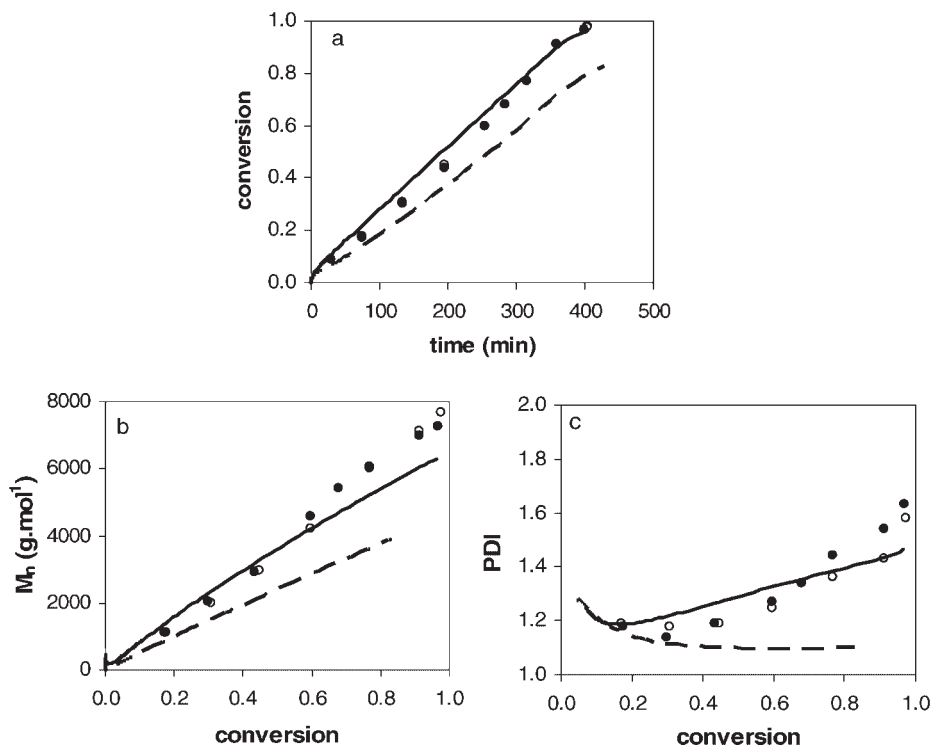


**Figure 4.**

Results from semibatch butyl acrylate ATRP at 90 °C: (a) conversion vs. time; (b) number average MW vs. conversion; (c) PDI vs. conversion. Data points are measurements from two experiments; the dashed line are model predictions generated using Table 1 rate coefficients with  $k_p$  reduced by factor of 7; the solid line are model predictions setting initiator efficiency to 0.68 and Cu(II) solubility to  $0.003 \text{ mol} \cdot \text{L}^{-1}$ .

lower. Clearly, there are important differences between semibatch and batch operation at the same temperature that leads to a loss of MW control. The experimental MW values indicate that initiator efficiency is significantly less than unity, in contrast to the BA batch polymerization at 90 °C. Thus, an apparent initiator efficiency of 0.68 is introduced to the simulation. However, this modification will not capture the loss of control. Previously we have shown that decreasing the solubility limit for Cu(II) leads to an increased reaction rate and polydispersity.<sup>[3]</sup> Figure 4 shows the simulation results obtained when  $[\text{Cu(II)}]_{\text{max}}$  is set to  $0.003 \text{ mol} \cdot \text{L}^{-1}$ , a factor of two lower than used for the batch ATRP polymerization at 90 °C. This modification is reasonable, considering that the semibatch mixture contains a lower fraction of

BA compared to the batch system, decreasing Cu solubility. These two simple modifications to the set of rate coefficients now provide a good fit to the experimental results, including the increase in PDI.

To improve control of the BA semibatch system, the reaction temperature was reduced to 70 °C. All other aspects of the process were kept identical to those at 90 °C. The results are shown in Figure 5. MW control is much improved than at 90 °C, with a final PDI of 1.1. The initiator efficiency is also higher, about 0.9. However, the polymerization rate is significantly reduced, with conversion only reaching 56% after 7 hours. Once again, the mechanistic model has been used to simulate these results, using the rate coefficients summarized in Table 1, with  $k_p$  reduced by a factor of 7 from the literature chain-end



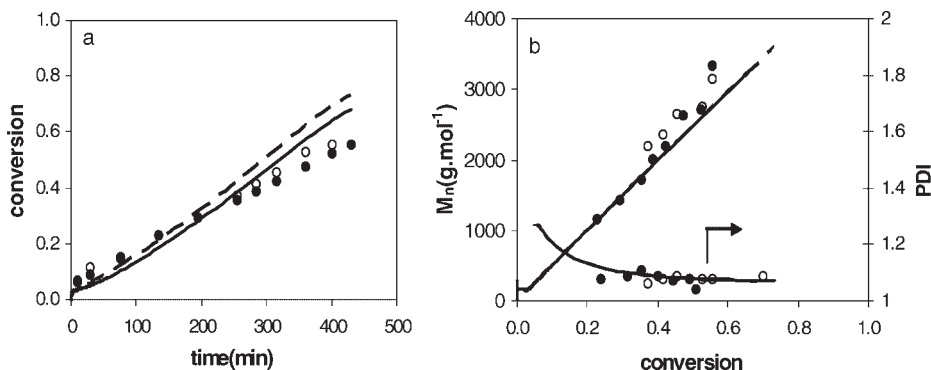


**Figure 5.**

Results from semibatch butyl acrylate ATRP at 70 °C (a) conversion vs. time; (b) number average MW and PDI vs. conversion. Data points are measurements from two experiments; the dashed lines are model predictions generated using Table 1 rate coefficients with  $k_p$  reduced by factor of 7; the solid lines are model predictions setting  $k_{act} = 0.5 \text{ L} \cdot \text{mol}^{-1} \cdot \text{s}^{-1}$ .

propagation value, to account for the presence of midchain radicals. In addition, operating at 70 °C will lower  $K_{eq}$ , due to a lower value for  $k_{act}$ . As shown in Figure 5, decreasing the value by 37.5% (from 0.8 to  $0.5 \text{ L} \cdot \text{mol}^{-1} \cdot \text{s}^{-1}$ ) provides a slightly better representation of conversion, without affecting  $M_n$  or PDI predictions.

Further optimization of semibatch operating conditions is required to find the best compromise between reaction rate and MW control. It is clear, however, that starved-feed operation of a semibatch reactor for ATRP BA homopolymerization can attain reaction rates comparable to a FRP system while maintaining good control, such that chains remain living throughout the entire semibatch monomer feeding period. This result indicates that it should be possible to manipulate composition along the polymer chain during copolymerization simply by varying monomer feed composition.

#### BA/Styrene Semibatch Copolymerization

LRP can be used to synthesize copolymers that range from random to block structure. Random copolymer, with constant (random) copolymer composition along the length of the chain, is the normal structure produced by FRP, but can also be produced by ATRP and other LRP techniques. The

living nature of ATRP produces copolymer with a well-defined molecular weight and narrow distribution, as well as a similar composition distribution along each chain. The monomer reactivity ratio and chemoselectivities in ATRP are very similar to those synthesized in conventional FRP, as expected for the radical process. For example, the reactivity ratios for the copolymerization of butyl acrylate/methyl methacrylate<sup>[12,25]</sup> and butyl methacrylate/methyl methacrylate<sup>[26]</sup> are the same for free radical and controlled radical copolymerization, independent of the structure of the catalyst complex.

For the ATRP semibatch copolymerization of styrene/BA, the weight ratio of monomer to solvent is kept at 70:30, and experiments were conducted at 110 °C. Styrene and BA were premixed at the desired ratio, then added to the reactor over a 6 h period, with 7% of the total monomer precharged to the reactor. Three random copolymerizations were conducted, with styrene/BA weight ratios of 25/75, 50/50 and 75/25. GC was used to analyze monomer concentrations of samples removed during the reaction, with copolymer composition calculated using material balances. There is reasonable agreement for the average molecular weights measured by GPC using the two detectors. For the RI



detector, molecular weights are calculated using a calibration curve established by narrow PDI polystyrene standards. As the Mark-Houwink parameters indicate, pBA calibration is very close to pS, therefore average molecular weights of copolymer from RI detector are used directly. For the LS detector, the  $dn/dc$  values were calculated using a composition-weighted average of the two homopolymer values. This procedure has been shown to be accurate for random copolymers,<sup>[6,27]</sup> but may not be appropriate for other structures; e.g., block and gradient copolymers. Thus, both RI and LS MW results are shown.

Figure 6 shows results for the experiment with styrene and BA at a 50/50 mass ratio. Conversion reached 81% after 8 hours and final  $M_n$  was  $7600 \text{ g} \cdot \text{mol}^{-1}$ , indicating an initiator efficiency of 0.50. This lower rate and lower efficiency is more typical of

styrene homopolymerization<sup>[3]</sup> than BA homopolymerization. This result can be understood in terms of relative radical fractions in the system: the majority of growing chains end in styrene radicals, as estimated by relative rates of cross-propagation. As a linear relationship is observed between number average molecular weight and conversion, it can also be concluded that most of the growing chains are lost at the beginning of the reaction. PDI of the copolymer remains below 1.3. Note that copolymer composition remains constant over the semibatch feeding time, indicating there is no composition gradient along the polymer chain. The experimentally measured monomer and polymer composition data for the three different monomer ratios can be plotted on a Mayo-Lewis representation, as shown by Figure 7. The curve shown is calculated

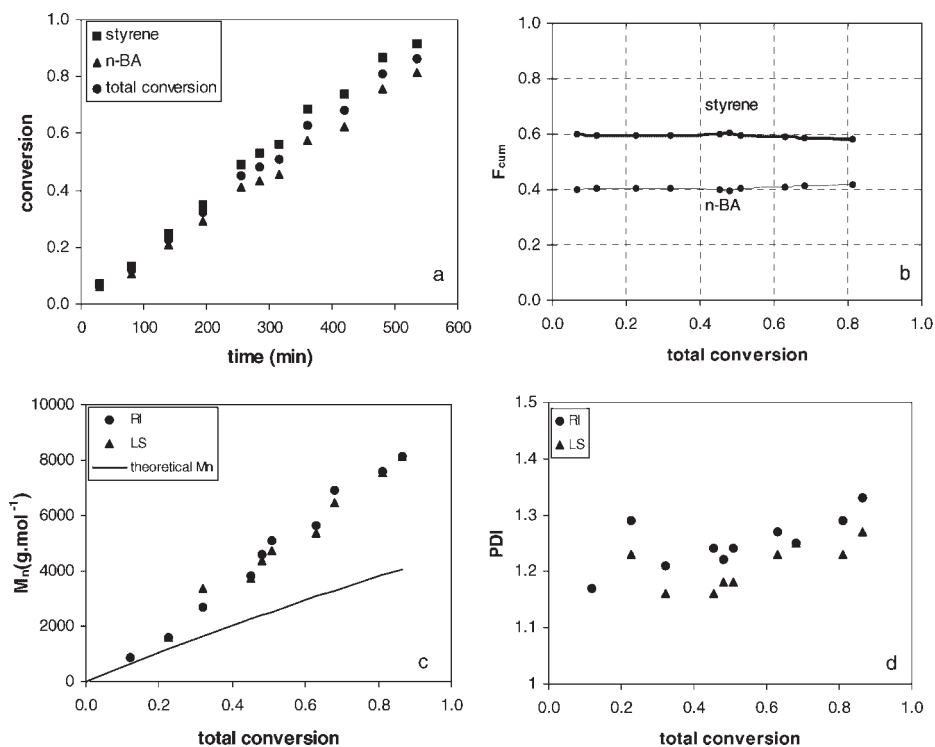


**Figure 6.**

Semibatch ATRP copolymerization at  $110^\circ\text{C}$  with styrene/butyl acrylate fed as a 50/50 wt mixture: (a) conversion vs. time; (b) cumulative polymer molar composition vs. conversion; (c) number average MW vs. conversion; (d) PDI vs. conversion.

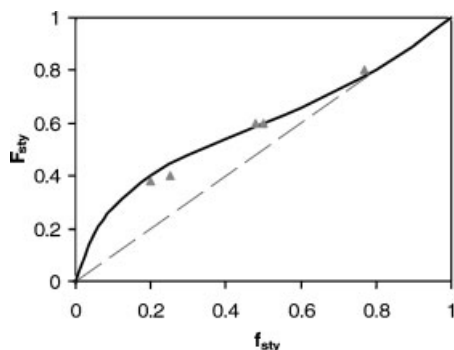


**Figure 7.**

Mole fraction of styrene incorporated in copolymer ( $F_{sty}$ ) vs. mole fraction of styrene in the monomer phase ( $f_{sty}$ ) for ATRP semibatch styrene/butyl acrylate random copolymerization. Data points from semibatch copolymerizations, with the curve calculated with  $r_{st} = 0.8$  and  $r_{BA} = 0.2$ .

according to literature reactivity ratios measured for a free radical polymerization system,  $r_{st} = 0.8$  and  $r_{BA} = 0.2$ .<sup>[28,29]</sup> There is a very good fit between three different monomer feeding ratio experimental data and the Mayo-Lewis equation generated using these reactivity ratios, indicating that ATRP copolymer composition is controlled by the same relative reactivities as in FRP, as expected for a radical process. The good agreement also indicates that the material balance procedures used to estimate polymer composition in the semibatch system are accurate.

Gradient copolymers have a continuous change in instantaneous composition along the polymer chain that can give the copolymer unique physical, thermal and mechanical properties, different from those of block and random copolymers. They can still show microphase separation,<sup>[30]</sup> but

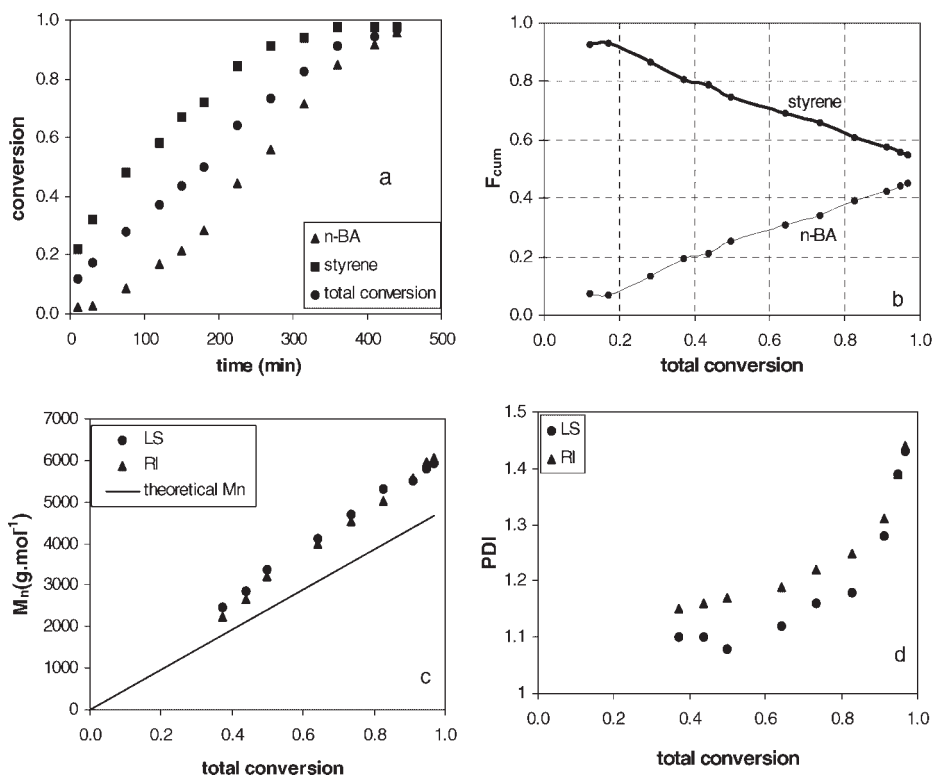


**Figure 8.**

Semibatch gradient copolymerization at 110 °C with continuous addition of butyl acrylate to a precharge containing styrene: (a) conversion vs. time; (b) cumulative polymer molar composition vs. conversion; (c) number average MW vs. conversion; (d) PDI vs. conversion.

with a lower order-disorder temperature than block copolymers, with potential applications as new blend compatibilizers and pressure sensitive adhesives.<sup>[30,31]</sup> This structure cannot be achieved by FRP but is possible with LRP; as all chains are initiated at the same time and live until the end of polymerization, the gradient in copolymer composition can be readily achieved by semibatch monomer feeding,<sup>[31]</sup> the strategy employed in this work. The overall recipe is the same as for the random copolymerization, with an equal mass ratio of styrene and BA. However, to produce the gradient structure, all of the styrene was added to the reactor precharge, with BA fed by semibatch addition over 3 hours after the precharge mixture (including initiator, CuBr and ligand) had reached 110 °C.

The results from this feeding strategy are shown in Figure 8. Continuously adding BA to the polymerization system creates an obvious composition gradient along the polymer chain, with styrene predominant first and composition becoming enriched in BA at the end of chain. The polymerization rate is reasonably fast, with conversion reaching 95% after 7 hours. Initiator efficiency is high, about 0.75. PDI is lower than 1.3 until almost complete conversion is reached, at which point the increase in PDI can be attributed to some loss of control during BA homopolymerization; styrene is almost completely consumed by this point in the reaction.

The opposite procedure of adding styrene to a BA precharge resulted in a block rather than a gradient copolymer, as shown

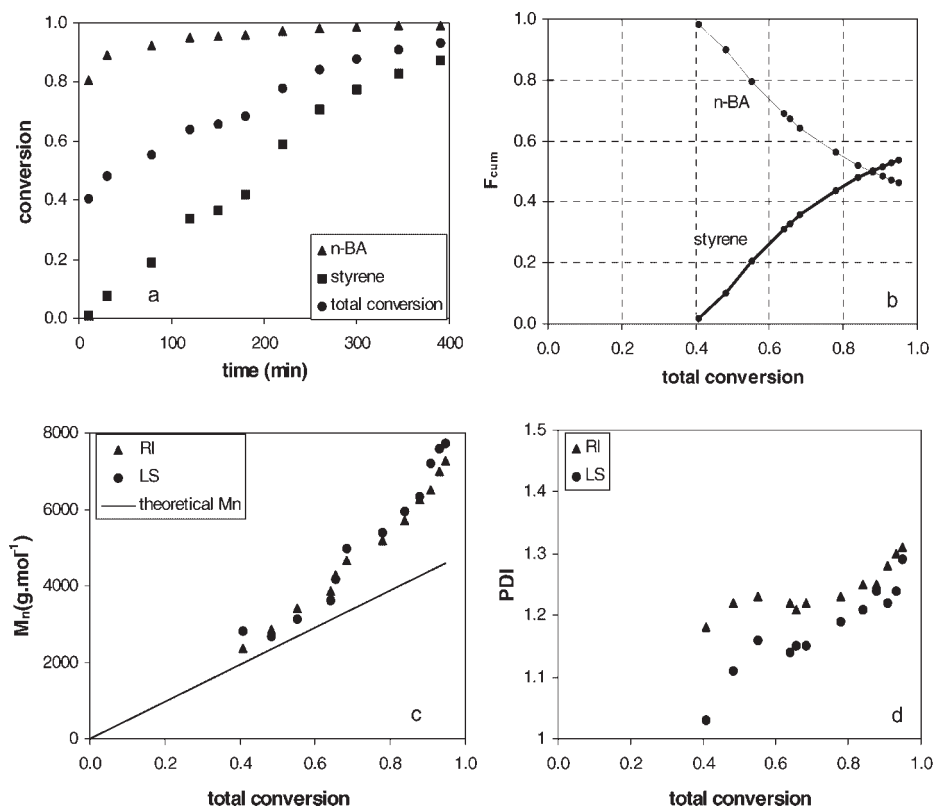


**Figure 9.**

Semibatch block copolymerization at 110 °C with continuous addition of styrene to a precharge containing butyl acrylate: (a) conversion vs. time; (b) cumulative polymer molar composition vs. conversion; (c) number average MW vs. conversion; (d) PDI vs. conversion.

in Figure 9. The precharge of BA already reached relatively high conversion as the reactor was being heated to 110 °C before styrene addition commenced. Thus the chains consist of a BA block followed by a block of predominantly styrene containing a small amount of BA. Higher polymerization rate and lower PDI is also obtained for styrene addition to BA, compared to BA addition to styrene. Conversion above 90% is reached in less than 6 hours and PDI remains lower than 1.3. Initiator efficiency is reduced, but is still higher than 0.6. This operating procedure is an effective one-pot method to produce a block copolymer, taking advantage of the much faster BA polymerization rate compared with styrene. With knowledge of the ATRP homopolymerization behavior of the two monomers, it is possible to select feeding profiles to make random, gradient, or block copolymers.

## Conclusion

BA batch and semibatch ATRP experiments were run at 90 °C, a lower temperature than that required for styrene polymerization. The system exhibited rapid polymerization rate (approaching that of FRP) and high initiator efficiencies. However, while good MW control was achieved in batch, it was necessary to reduce temperature to 70–80 °C to maintain control during semibatch operation. The loss of control during semibatch operation can be explained by a decrease in Cu solubility during the course of the reaction. A mechanistic model, using BA rate coefficients from literature and the solubility data from this study, provides a good representation of the ATRP experimental results after decreasing  $k_p$  to about 1/7 of the chain-end literature value to account for reduced rate due to the production of midchain radicals from intramolecular chain transfer.

ATRP has also been shown to be effective for the synthesis of random, gradient and block styrene/BA copolymers

at 110 °C, with the chain microstructure controlled by the addition strategy used in the semibatch process. Random copolymers of various composition were produced by adding both monomers simultaneously; the starved-feed strategy resulted in constant polymer composition with no gradient along the polymer chain, matching the structure that would be produced by starved-feed FRP copolymerization. The copolymer composition data for these random copolymers are well-represented by literature reactivity ratios for FRP. A gradient copolymer was polymerized at the same conditions as the random copolymers, with the only change being that all of the styrene was precharged to the system, and BA was fed over time. Block copolymer was produced by precharging BA to the system, and feeding styrene over time. All of the above copolymerizations were conducted with good MW control ( $PDI < 1.4$ ), and reasonable reaction rates. These results illustrate the potential of ATRP to manipulate chain microstructure while producing copolymers of controlled composition and MW with narrow PDI using a semibatch reactor system.

**Acknowledgements:** We thank the Natural Sciences and Engineering Research Council of Canada for financial support of this work.

- [1] Y. Wang, R. A. Hutchinson, M. F. Cunningham, *Macromol. Mat. Eng.* **2005**, 290, 230.
- [2] Y. Fu, M. F. Cunningham, R. A. Hutchinson, *Macromol. React. Eng.* **2007**, 1, 243.
- [3] Y. Fu, A. Mirzaei, M. F. Cunningham, R. A. Hutchinson, *Macromol. React. Eng.* **2007**, 1, 425.
- [4] M. Müller, M. F. Cunningham, R. A. Hutchinson, *Macromol. React. Eng.* **2007**, accepted.
- [5] S. Beuermann, D. A. Paquet, Jr., J. H. McMinn, R. A. Hutchinson, *Macromolecules* **1996**, 29, 4206.
- [6] J. C. Seferis, *Refractive Indices of Polymers*, in: *Polymer Handbook*, 4th ed., J. Brandrup, E. H. Immergut, E. A. Grulke, Eds., John Wiley & Sons, New York **1989**.
- [7] D. A. Shipp, K. Matyjaszewski, *Macromolecules* **2000**, 33, 1553.
- [8] A. Snijder, B. Klumperman, R. Linde, *Macromolecules* **2002**, 35, 4785.
- [9] S. Faucher, S. Zhu, *Macromol. Rapid Commun.* **2004**, 25, 991.

- [10] S. Faucher, S. Zhu, *Macromolecules* **2006**, 39, 4690.
- [11] J. Queffelec, S. G. Gaynor, K. Matyjaszewski, *Macromolecules* **2000**, 33, 8629.
- [12] M. J. Ziegler, K. Matyjaszewski, *Macromolecules* **2001**, 34, 415.
- [13] J. M. Asua, S. Beuermann, M. Buback, P. Castignolles, B. Charleux, R. G. Gilbert, R. A. Hutchinson, J. R. Leiza, A. N. Nikitin, J.-P. Vairon, A. M. van Herk, *Macromol. Chem. Phys.* **2004**, 205, 2151.
- [14] S. Beuermann, M. Buback, *Prog. Polym. Sci.* **2002**, 27, 191.
- [15] A. N. F. Peck, R. A. Hutchinson, *Macromolecules* **2004**, 37, 5944.
- [16] S. Maeder, R. G. Gilbert, *Macromolecules* **1998**, 31, 4410.
- [17] H. Fischer, H. Paul, *Acc. Chem. Res.* **1987**, 20, 200.
- [18] Y. Fu, *PhD Thesis*, Queen's University, Kingston, Ontario, Canada **2007**.
- [19] K. Davis, H.-J. Paik, K. Matyjaszewski, *Macromolecules* **1999**, 32, 1767.
- [20] J. Xia, K. Matyjaszewski, *Macromolecules* **1997**, 30, 7697.
- [21] C. Plessis, G. Arzamendi, J. R. Leiza, H. A. S. Schoonbrood, D. Charmot, J. M. Asua, *Macromolecules* **2000**, 33, 4.
- [22] M. Bednarek, T. Biedron, P. Kubisa, *Macromol. Chem. Phys.* **2000**, 201, 58.
- [23] J. Huang, T. Pintauer, K. Matyjaszewski, *J. Polym. Sci., Part A: Polym. Chem.* **2004**, 42, 3285.
- [24] R. Sharma, A. Goyal, J. Caruthers, Y. Won, *Macromolecules* **2006**, 39, 4680.
- [25] S. G. Roos, A. H. E. Müller, K. Matyjaszewski, *Macromolecules* **1999**, 32, 8331.
- [26] D. M. Haddleton, M. C. Crossman, K. H. Hunt, C. Topping, C. Waterson, K. G. Suddaby, *Macromolecules* **1997**, 30, 3992.
- [27] D. Li, N. Li, R. A. Hutchinson, *Macromolecules* **2006**, 39, 4366.
- [28] G. Chambard, B. Klumperman, A. L. German, *Polymer* **1999**, 40, 4459.
- [29] S. V. Arehart, K. Matyjaszewski, *Macromolecules* **1999**, 32, 2221.
- [30] T. Pakula, K. Matyjaszewski, *Macromol. Theory Simul.* **1996**, 5, 987, 4459.
- [31] K. Matyjaszewski, M. J. Ziegler, S. V. Arehart, D. Greszta, T. Pakula, *J. Phys. Org. Chem.* **2000**, 13, 775.